Reversible redox modifications in microglia proteome challenged by beta amyloid

Virginia Correani[a], Laura Di Francesco[a] , Isabella Cera[a‡], Giuseppina Mignogna[a], Alessandra Giorgi[a], Michele Mazzanti[b], Lorenzo Fumagalli[c], Cinzia Fabrizi[c], Bruno Maras[a] and M.Eugenia Schininà*[a]

[a] Dipartimento di Scienze Biochimiche, Sapienza University of Rome, Rome, Italy

[b] Dipartimento di Bioscienze, Università degli Studi di Milano, Milan, Italy

[c] Dipartimento di Scienze Anatomiche, Istologiche, Medico-Legali e dell'Apparato Locomotore, Sapienza University of Rome, Rome, Italy

* Corresponding author: Prof. M. Eugenia Schininà
Dipartimento di Scienze Biochimiche
Sapienza University of Rome
Piazzale Aldo Moro, 5
00185 Rome
Italy
email address: eugenia.schinina@uniroma1.it
Phone: +39 06 49910605
Fax: +39 06 4440062

‡ Current address: Institute for Neuroscience, Medical University of Innsbruck, Innsbruck, Austria

This paper is dedicated to the memory of our beloved collegue, prof. Donatella Barra, unforgettable guidance in science and life.

Abstract

Microglia are resident macrophages in the central nervous system, whose engagement against exogenous injuries and infections is mainly marked by an immediate release of inflammatory cytokines along with a toxic efflux of superoxide radicals. Indeed, many lines of evidence indicate that a persistent activation of these cells turns their neuroprotective phenotype toward a neutotoxic one, which does contribute to dismantle neuronal activity and to induce neuronal loss in several neurodegenerations, as in the Alzheimer's disease. In this study we addressed to fill in the gap in our knowledge about redox regulation of amyloid activated microglia. With this aim, we carried out a robust and comprehensive characterization of the reversibly redox modified proteome both at the level of resting and of amyloid-activated BV2 cells, an immortalised line of murine microglia. The approach we used combined a selective enrichment of reversible redox modified proteins through a biotin bait with nanoscale liquid chromatography tandem mass spectrometry of their proteolytic peptides. By this reliable approach, we identified 60 proteins changing the redox status of their selective cysteine residues upon treatment with the amyloidogenic $A\beta_{25–35}$ peptide. These results assessed that in microglia stimulated by amyloids, redox modifications of proteome specifically target proteins involved in crucial cell processes, *i.e.* those involved in the protein synthesis. In particular, for peroxiredoxin-6 (Prdx6) and Ras-related C3 botulinum toxin substrate 1 (Rac1) we suggest mechanisms through which reversible redox modifications could affect the peculiar microglia role in the amyloidogenic injury, that is at the same time to reinforce the oxidative burst and to resist toward it. Moreover, the redox modulation we observed on chloride intracellular channel protein 1 (CLIC1) strengthens the structural and functional relationships between the oxidative stress and the metamorphic transition of this protein from a soluble to an integral membrane form. The redox signatures we determined might also provide neurologists with more specific and reliable biomarkers to distinguish diverse microglia status in neurodegenerations and then to drive targeted drug designing.

Introduction

Alzheimer's disease (AD) is an age-related neurodegenerative disorder characterized by a progressive loss of neurons and synapses, mostly in the cerebral cortex.[1] In AD, molecular hallmarks of neuronal damage are both intracellular aggregates of hyperphosphorylated Tau protein and extracellular insoluble fibres made up by beta-amyloid (Aβ) peptides, released by the sequential cleavage of the membrane Amyloid Precursor Protein (APP) by beta and gamma secretases.[2] However, only the Aβ soluble oligomers precursors of the insoluble fibres have been proved to be neurotoxic, and therefore regarded as the main aetiological agent in AD neurodegeneration.[3] Although the precise mechanisms by which Aβ peptides trigger neurodegeneration remain unclear, one of the established biochemical features of AD injured tissues is an unbalanced cellular redox state, mainly touched off in the glial compartment.[4, 5]

Microglia are resident macrophages of the central nervous system that play an essential role in homeostasis maintenance, tissue repair, innate immunity response and neuroinflammation.[6] In response to injuries and infections these cells are able to release inflammatory cytokines along with toxic efflux of superoxide radicals produced by the NADPH oxidase complex.[7] Although upon this oxidative burst the extracellular environment becomes strongly oxidative, the microglia themselves are able to proliferate and differentiate. Therefore, microglia should be considered cells intrinsically resistant to oxidative stress.

However activated microglia do not constitute a unique cell population.[8, 9] Upon any homeostatic disturbance that may challenge the neuronal compartment (ranging from cell debris to diverse toxins), quiescent microglia, in a tight cross-talk with neurons and astrocytes, are known to assume a diversity of reactive states to alternatively prime debris clearance, tissue repair or neuronal death.[10] With the aim to discover therapeutics agents selectively targeting toward the neurotoxic state(s), nowadays much effort has been put in identifying biomarkers which can distinguish different microglia states.[11, 12] The neurotoxic state of microglia in AD is reasonably pushed by the oxidative stress and thus studies dedicated to identify changes in the proteome redox states may

help in designing targeted therapies.

Protein cysteinyl residues are among the possible sensitive sites of an altered concentration of redox metabolites. Although cysteine is one of the least abundant amino acids in proteome, this residue often plays a pivotal role in the fragile equilibrium between protein folding and misfolding. When under an oxidative stress the intracellular environment switches from a reductive to an oxidative state, cysteines at the protein surface may stochastically form intermolecular disulfide bridges, leading to intracellular proteinaceous polymers which in turn may impair cell functions. In this scenario, any post-translational modification of cysteinyl residues may play a key role in protecting intracellular proteins from these irreversible modifications.[13] Nonetheless, recent evidences show that reversible post-translational modification of cysteines, like the covalent binding of glutathione (GSH) by S-glutathionylation and of nitric oxide (●NO) moiety by S-nitrosylation, may represent a key step in protein functional regulation and cell signalling.[14, 15] Indeed, the presence inside the cell of enzymes able to catalyse protein trans-glutathionylation and trans-nitrosylation (*e.g.* glutathione S-transferases, S-nitrosoglutathione reductase, glutaredoxin and thioredoxin system) suggests that these reversible redox modifications (hereafter RRMs) may give rise to molecular networks similar to that generated by protein phosphorylation/dephosphorylation.[16, 17] In turn, the occurrence of modifications of cysteinyl residues by S-glutathionylation and S-nitrosylation is emerging as a key step in neurodegenerative diseases, as well as in other chronic pathologies like type 2 diabetes and multiple sclerosis.[18-20]

In AD, the knowledge of the roles of S-glutathionylation and S-nitrosylation is only at the beginning.[21-23] Technical difficulties in “trapping” into cell lysates the thiol states of cysteinyl residues and in avoiding disulfide shuffling during proteome manipulations may explain the paucity of the available data. In this study, we investigated in microglia the effects of amyloid peptides on the redox state of the proteome cysteinyl residues, generally referred to as redox-proteome.[24] For this purpose, we applied on a microglia cell culture upon amyloid treatment a targeted strategy for a proteome-wide identification of cysteinyl residues that undergo a reversible oxidation.[25] With the

results achieved, we suggest a role for RRMs in triggering microglia towards the activated phenotype responsible for neuroinflammation in AD.

Material and Methods

Chemical and materials

BV2 cells is an immortalised murine microglia cell line, continuously maintained at the Dipartimento di Scienze Anatomiche, Istologiche, Medico-Legali e dell'Apparato Locomotore, from an original gift of prof. Giulio Levi (Istituto Superiore di Sanità, Rome). Dulbecco's Modified Eagle Medium, fetal calf serum, penicillin, streptomycin and glutamine were from Sigma-Aldrich. The $A\beta_{25-35}$ (GSNKGAIIGLM) peptide was from Bachem (AG, Bubendorf, Switzerland). Ammonium bicarbonate, ß-mercaptoethanol, urea, 3-[(3-cholamidopropyl)dimethylammonio]-1-propanesulfonate (CHAPS), sodium chloride, N-ethyl maleimide (NEM) were purchased from Sigma-Aldrich (St. Louis, MO, USA). Ethanol, water, acetonitrile (ACN), formic acid (FA) were purchased from Fluka Chemie (AG, Buchs, Switzerland). Potassium chloride, dibasic sodium phosphate and monobasic potassium phosphate were purchased from Merck KGaA (Darmstadt, Germany). From Bio-Rad (Hercules, CA, USA) were purchased Tris-HCl, dithiothreitol, Triton X-100 and the Bradford reagent. Protease inhibitor cocktail (Complete, mini Protease inhibitor cocktail tablet) was supplied by Roche (Mannheim, Germany). EZ-link N-[6-(biotinamido)hexyl]-3'-(2'-pyridyldithio)propionamide-biotin and high capacity streptavidin-agarose resin were purchased from Thermo-Scientific Pierce (Rockford, IL, USA). Trypsin was purchased from Promega (Madison, WI, USA). C_{18} reverse-phase loaded Empore™ SPE disks were from Sigma-Aldrich. Fused silica capillaries were from New Objective (Woburn, MA, USA), and C_{18} reverse-phase beads from Michrom Bioresources (Auburn, CA, USA). All aqueous solutions were prepared with ultrapure water (18.2MΩ/cm) from Milli-Q water purification system (EMD Millipore, Billerica, MA, USA).

Cell cultures

The murine microglial cell line BV2,[26] were grown in Dulbecco's modified Eagle's medium (DMEM) supplemented with 100 U/ml penicillin, 100 µl/ml streptomycin, 10% fetal calf serum and 2 mM L-glutamine; cultures were maintained at 37 °C in 5% CO_2/95% humidified air atmosphere. Synthetic $A\beta_{25–35}$ (GSNKGAIIGLM) peptides was dissolved in sterile, distilled water at a concentration of 1 mM and incubated for 72 h at 37°C to allow aggregation.[27]

BV2 cells were cultured in 75 cm^2 culture flask at a density of $5x10^6$ cells/flask, washed with serum-free media, and challenged with 50 µM $A\beta_{25-35}$ peptide for 24 h.

Isolation of the reversibly oxidized thiol-containing proteins.

Three replicates each for $A\beta_{25-35}$ treated and untreated (control) BV2 cells were harvested, washed twice with phosphate buffer saline (PBS) containing 1.37 M NaCl, 27 mM KCl, 100 mM Na_2HPO_4, 18 mM KH_2PO_4, and lysed in an alkylating buffer containing 8 M urea, 100 mM N-ethyl maleimide (NEM), 50 mM Tris-HCl pH 8.0, 0.1% Triton X-100 and the required amount of the protease inhibitor cocktail according to the manufacturer's instructions. After incubation under rotation at 4°C for 30 min, three cycles of sonication/relaxation of 30 s were carried out. Protein concentration for each sample was then measured using Bradford reagent and bovin serum albumin (BSA) as a standard.

Proteins with a reversible oxidation on cysteinyl residues were selectively isolated from these samples using the "biotin switch" approach, as further implemented by McDonagh *et al.*[25] and slightly modified for a better recovery of proteins. In brief, equal aliquots (500 µg of proteins) from each lysate obtained from the three replicates of untreated and $A\beta_{25-35}$ treated BV2 cells were precipitated overnight at -20°C with nine volumes of cold ethanol and protein pellet collected by centrifugation at 14,000 rpm at 4°C for 15 min to remove the excess of NEM. Reduction of reversibly oxidised cysteinyl residues was then performed re-dissolving all these pellets in 180 µl of

a strongly reducing buffer containing 8 M urea, 4% CHAPS, 50 mM Tris-HCl pH 8.0 and 2 mM ethylenediaminetetraacetic acid (EDTA), adding dithiothreitol (DTT) to a final concentration of 20 mM, and incubating for 45 min on a rotator at room temperature. DTT removal was performed by ethanol-precipitation of the protein fraction. Protein thiols have finally been alkylated with a buffer (200 µl) containing a large excess of N-[6-(biotinamido)hexyl]-3'-(2'-pyridyldithio)propionamide (HPDP)-biotin (0.5 mM) for 45 min on a rotator in the dark. After removal of the unbound HPDP-biotin reagent again by ethanol precipitation, equal aliquots of each protein mixture (200 µg) were proteolysed at 37°C overnight with 200 µl of a solution of sequencing grade trypsin (1:50 E/S, w/w) in 50 mM ammonium bicarbonate containing 0.8 M urea. Proteolysis was stopped by adding 200 µl of the denaturing buffer, free of DTT.

Affinity resin was prepared by washing twice an appropriate quantity of slurry streptavidin-agarose resin in a binding buffer containing 4 M urea, 2% CHAPS, 25 mM Tris-HCl pH 8.0 and 50 mM NaCl. Aliquots of 40 µl of resin (50% slurry) were then incubated with each tryptic peptide mixture at 4°C overnight on a rotator. After centrifugation at 5,000 rpm, each supernatant containing the unbound peptides was re-incubated with fresh streptavidin-agarose resin, and pooled with the previous resin fraction. The resin samples obtained were washed stepwise with equal volumes (200 µl) of a) the binding buffer, b) a buffer containing 8 M urea, 4% CHAPS, 25 mM Tris-HCl pH 8.0, 1 mM NaCl (two washes), c) the same buffer without 1 mM NaCl (two washes), and d) a buffer containing 5mM ammonium bicarbonate and 20% acetonitrile (ACN; two washes). Peptides from the insoluble resin were finally released by exchange the S-linked biotin-cysteinyl residues to ß-mercaptoethanol cysteinyl adducts with a treatment for 5 min at 56°C with a buffer (25 µl) containing 5mM ammonium bicarbonate, 20% ACN, and 5% ß-mercaptoethanol. Released peptides were collected by centrifugation at 5,000 rpm and supernatants stored at -80°C.

With the aim to assess possible unspecific interactions, minimal aliquots from all the six cell lysates were pooled, and then challenged with streptavidin-agarose beads in the same conditions used for the affinity isolation of peptides containing reversibly modified cysteines described above.

Protein Identifications

Each of the six peptide mixtures, three biological replicates from resting and three from $A\beta_{25-35}$ treated BV2, was divided in two equal amount for technical replica (Fig. 1). All these twelve samples were analysed by nano-liquid chromatography hyphenated with tandem mass spectrometry (LC-MS/MS) on an Ultimate3000 system (Dionex, Sunnyvale, CA, USA) equipped with a splitting cartridge for nanoflows and connected *on-line via* a nanoelectrospray ion source (Thermo-Fisher Scientific, Waltham, Massachussetts, USA) to an LTQ-Orbitrap XL mass spectrometer (Thermo-Fisher Scientific).

Samples were preliminarily desalted using C_{18} reverse-phase loaded Empore™ solid phase extraction (SPE) disks, according to the StageTip protocol,[28] resuspended in 0.1% formic acid (FA) and automatically loaded from the autosampler module of the Ultimate 3000 system onto a 10 cm long silica capillary (360 μm o.d., 75 μm i.d. fused silica with a 8 μm i.d. tip, New Objective, Woburn, MA, USA) handmade packed with C_{18} reverse phase resin (Magic C_{18}AQ, 5 μm particle, 200 Å pore size), equilibrated in 95% solvent A (5% ACN, 0.1% FA) and 5% solvent B (80% ACN, 0.1% FA). According to the expected complexity, peptide mixtures were fractioned by elution with a 5-80% gradient of solvent B over 110 min at a 300 nl/min flow rate obtained by a flow split ratio of 1:1000.

As peptides were eluted, they were electrosprayed directly into the mass spectrometer with an electrospray (ESI) voltage of 1.9 kV. Mass spectral (MS) data were acquired in a positive mode in the Orbitrap in Fourier Transforming Ion Cyclotron Resonance Mass Spectrometry (FTMS) mode over 300-2000 *m/z* range with resolution 30,000 at *m/z*=400, with an automatic gain control (AGC) target of 1×10^6 ions, and the maximal injection time of 1000 ms. Tandem mass spectra (MS/MS) were acquired into the linear ion trap quadrupole (ITMS) by data-dependent mode with the Xcalibur™ software, selecting the five most intense ions with charge states ≥ 2 detected *per* survey scan by FTMS, through collision-induced dissociation (CID), and analysing the resulting fragments

in the linear trap (LTQ). LTQ was calibrated using an calibrating mixture (LTQ ESI Positive Ion Calibration Solution Spectra; Thermo-Fisher Scientific) with the following formulation: caffeine (20μg/ml), peptide with sequence Met-Arg-Phe-Ala (1μg/ml) and Ultramark 1621 (0.001%) in an aqueous solution of acetonitrile (50%), methanol (25%) and acetic acid (1%). For MS/MS scanning, the minimum MS signal was set to 500, activation time to 30 ms, target value to 10,000 ions, and injection time of 100 ms. All MS/MS spectra were collected using a normalized collision energy of 35% and an isolation window of 2 Th. To avoid redundant sequencing of the most abundant peptides, dynamic exclusion was enabled with a repeat count of 1, a repeat duration of 30 s, an exclusion list size of 300 and an exclusion duration of 90 s.

Data analysis

All mass spectrometric data were analysed by the proteomics software package MaxQuant (version 1.3.5).[29] MS/MS spectra were searched against the *Mus musculus* dataset of UniprotKB database (release 2014_02; 51,373 sequences). Trypsin was selected as cleavage enzyme. A maximum of two missed cleavages and +4 charge states were allowed for detected peptides. Mass tolerance for FTMS and for ITMS measurements were respectively set to 20 ppm and 0.5 Da. The False Discovery Rate (FDR) was set to 0.005 (0.5%) at protein and peptide levels. The following variable modifications were also used in identification: oxidation of methionine, deamidation of asparagine and glutamine, cysteine with mercaptoethanol and NEM. Peptides with a length less than 7 were automatically rejected. Matching of 2 min between runs and a minimum ratio count of 1 were set. Searches were also achieved against both a dataset of commonly detected contaminants in proteomics and the reverse decoy database generated by the Andromeda search engine, and identified peptides manually removed. Protein identifications by only one peptide were manually validated according to Mann *et al.*[30] Moreover, all peptides that were demonstrated a) to aspecifically interact with streptavidin-agarose beads, b) not to comprise cysteinyl residues in their sequence, c) not to be ascribable either to a protein group unique or to a single gene product, were

manually removed from the list. Reversibly redox-modified cysteinyl-containing peptides not identified in at least one technical replicas of each of the three biological replicates were rejected. Assignment of a protein function annotation and clustering of the detected proteins according to molecular and cellular functions were performed using the Ingenuity Pathway Analysis (IPA; www.ingenuity.com). The analysis of enrichment in protein function and cellular processes were based on information contained in the Ingenuity Pathways Knowledge Bases. The statistical significance of these enrichments was evaluated by Fisher's exact test.

Total RNA preparation and real-time polimerase chain reaction (RT-PCR)

After the 4 h treatment with $A\beta_{25-35}$, total RNA was purified by $2x10^6$ BV2 cells by a single extraction with Trizol (Invitrogen) and reverse transcribed by oligo$(dT)_{15-18}$ primers and MML-V reverse trascriptase (Invitrogen). The cDNA was amplified by Taq DNA polymerase in a thermal cycle (PerkinElmer Life Sciences) in the presence of primers for tumor necrosis factor (TNF-α) (5'-primer, GAGCACTGAAAGCATGATCCG; 3'-primer GCAGGTCTACTTTGGGATCATT). Conditions for TNF-α amplifications were as follows: 30 s at 94°C, 30 s at 64°C, 30 s at 72°C. Ten microliters of each PCR product were electrophoresed on 1% agarose gel and then visualized by ethidium bromide staining. The mRNA for glyceraldehyde 3-phosphate dehydrogenase (GAPDH) was used as reference.

Western blot analysis

Protein extracts (approximately, 20 μg) were resolved by 12% sodium dodecyl sulfate (SDS)-polyacrylamide gel electrophoresis (SDS-PAGE; 200V, 45min). Protein bands were electrotransferred to nitrocellulose membranes (80 mA, 45min). Membranes were then treated with 5% enhanced chemiluminescence (ECL) blocking agent (GE Healthcare Bio-Sciences) in a saline buffer (T-TBS) containing 0.1% Tween-20, 10 mM Tris-HCl, 150 mM NaCl, 1 mM $CaCl_2$, and 1 mM $MgCl_2$, pH 7.4, for 1 h and then incubated with primary antibody overnight at 4°C.

Subsequently, membranes were washed three times in T-TBS, and bound antibodies were detected using appropriate horseradish peroxidase-conjugated secondary antibodies, followed by an ECL Plus Western blotting Detection System (GE Healthcare Bio-Sciences). ECL was detected using a Molecular Imager® ChemiDoc™ mod. MP System (Bio-Rad Laboratories), and acquired by ImageLab Software ver. 4.1. Immunodetections were carried out using rabbit polyclonal antibodies (Santa Cruz Biotechnology) against Ras-related C3 botulinum toxin substrate 1 (Rac1; sc-217, dilution 1:500), chloride intracellular channel protein 1 (CLIC1; sc-134859, dilution 1:800), peroxiredoxin-6 (Prdx6; sc-134478, dilution 1:200) and against cytokine- inducible nitric oxide synthase (anti-iNOS/NOS-II; Transduction Laboratories 610332, dilution 1:10000) proteins. In each analysed sample, signal of the target protein was normalized to the corresponding GAPDH (Santa Cruz Biotechnology, sc-32233; antibody dilution 1:500) or β-tubulin (Sigma-Aldrich, T8328; dilution 1:10000) level, which show a comparable expression levels both in treated and untreated cells (Fig. 1S). Three replicates were performed, one for each biological sample. All results are expressed as mean ± SD. Differences between experimental groups were determined by Student's t-test. *p*-value of <0.01 were considered statistically significant.

Cell viability

Lactate dehydrogenase (LDH) release in the culture medium was measured using a cytotoxicity detection kit (Roche, Mannheim, Germany) according to the manufacturer's protocol.

Results

With the aim of providing selective targets of the oxidative stress in microglia injured by beta amyloid, in this study we approached the identification of reversible redox modified (RRM) cysteinyl residues by mass spectrometry-based proteomics.

Although redox-proteomics is an emerging field in neurobiology, it is a very difficult issue from a

methodological point of view. Perhaps the main problem is represented by the requirement to stabilize the proteome thiols against artefactual oxidation.[31] This aim is particularly challenging in 2DE-gel based proteomics, where the high number of sample manipulation steps cause poorly reproducible assessments of the thiol states of protein spots. To overcome this problem, a significant number of techniques based on resin-assisted enrichment of cysteine-containing proteome have been proposed.[reviewed in 32-34] According to one of these approaches, named "biotin switch", immediately after the cell lysis specific RRMs (*e.g.* S-nitrosylation, S-glutathionylation, disulfide bridges) are selectively tagged with biotin-derivatives containing a disulfide bridge.[25] The entire proteome was then proteolysed and biotin-containing peptides were selectively isolated by a streptavidin-based affinity step. According to this methodological pipeline, the "biotin-switch" has recently provided a reliable evaluation of the redox states of the erythrocytes proteins when coupled with shotgun proteomics.[35]

We applied this approach (schematically summarised in Fig. 1) to BV2 cells, the most frequently used cellular model for microglia in proteomics.[36, 37] We treated BV2 with $A\beta_{25-35}$, a shorter and a more manageable form of the full-length $A\beta_{1-42}$ peptide, known to be able to induce inflammatory and oxidative status on microglia, without affecting cell viability (Fig. 2).[11, 38-42]

The high degree of selectivity of the "biotin-switch" strategy we employed was proved both by the absence of capturing activity against microglia lysates as well as by the high percentage of cysteinyl-containing peptides captured (91%). Moreover, the high yield of the strategy was assessed by the finding in the shotgun proteomics of $A\beta_{25-35}$ treated and untreated cells of a total of 1129 peptides. This number of peptides is in a good agreement with the redox-modified peptide pool baited in mouse macrophages by Su *et al.* upon treatment with exogenous oxidants.[43]

Since our aim was to identify a consistent peptide panel reliable to distinguish redox-modified proteins between resting and amyloid activated microglia, we considered only peptides uniquely assigned by proteomics to one protein and identified in at least one technical replica of all the three biological replicates of the microglia cultures used. These stringent comparison criteria yielded 287

peptides out of the 1129 identified. These peptides allowed a confident identification of a total of 193 proteins, even by only one reversible redox modified peptide captured as biotin adduct (Table S1, ESI†). To assess the biological processes and the protein functions possible affected by the acquisition of redox modifications on cysteinyl residues in microglia proteome, these 193 proteins were clustered into protein function (Fig. 3A) and biological processes (Fig. 3B) according to the Ingenuity Pathways Knowledge Bases.

A detailed analysis of redox modified peptides consistently captured by the biotin-streptavidin approach showed that for a large number of them (223 out of 287, 78%) the beta amyloid activation does not induce a change in the redox state. On the other hand, upon treatment with $A\beta_{25-35}$ peptide we observed a selective enrichment for 40 peptides and a selective missing of 24 redox modified peptides captured in the resting status (Table S2, ESI†). Indeed, according to the consistent shotgun proteomic identification we obtained, the beta amyloid treatment can induce selective gain or loss of reversible redox modifications on targeted cysteinyl residues for 36 and 21 proteins respectively (Table S2, ESI†). Moreover, an opposite pattern of oxidation for a couple of cysteines of the same protein could be observed for the subunit beta 2-like-1 of the guanine nucleotide-binding protein (RACK1) and for the heterogeneous nuclear proteins K and L (hnRNPK and hnRNPL). In these couple of residues for each of these three proteins, the former cysteinyl residue found redox modified in the resting cells lost the modification in the activated ones, whereas the latter cysteinyl gained the modification only in the activated form.

Aimed to validate the changes in the redox profiles we highlighted between resting and activated microglia cells, we ruled out the possibility that different protein expression levels between treated and untreated cells may affect our results. Particularly, we focused on three proteins possible linking oxidative stress with microglial neurotoxic activity, namely peroxiredoxin-6 (Prdx6), Ras-related C3 botulinum toxin substrate 1 (Rac1) and chloride intracellular channel protein 1 (CLIC1). By immunostaining we proved that the expression level of these three proteins did not change between resting and activated microglia, confirming that their redox modified variants appeared

only in the proteome of $A\beta_{25-35}$ stimulated microglia.

Discussion

The increasing interest in determining post-translational modifications as molecular switches towards alternative protein functions has recently encountered the investigation of the role of oxidative stress in chronic pathologies. In studies focused on redox-modifications of proteins, nitrosylation and glutathionylation gained a place of honour.[16, 18, 25]

In this paper, we investigated changes that in the redox landscape of microglia accompany beta amyloid exposure. To approach this issue, we took advantage from a fast and highly selective methodology, based on the biotin/streptavidin affinity system, and hyphenated with a MS-based proteomics. In particular, this platform was targeted to specifically isolate reversibly redox-modified peptides and thus allowed us to determine the precise cysteinyl residue whose redox states is modulated in the microglia proteome by oxidative stress.

Recent papers suggested that a limited (hundreds) but selective number of proteins are subjected to RRMs.[16] The results reported herein show that considering both the microglia states we addressed, the number of proteins found reversible redox modified (193) is in the same range as observed in other cellular models (see references in Table S2, ESI†). As evident from Fig. 3, our data indicate that in microglia RRMs target mainly proteome components involved in protein biosynthesis, that clustered ribosomal proteins, translational regulators and molecular chaperons, and in two other processes, *i.e.* cellular growth/proliferation and inflammation, on which peculiarly microglia biology is based.[12]

The differential analysis between resting and beta-amyloid activated microglia we provided herein allowed us to identify 60 proteins in which the redox state of the sensitive cysteinyl site(s) is consistently changed in the activated phenotype (Table S2, ESI†). Although some of these cysteinyl site(s) have been recently observed as reversible redox modified in other cell models (see references

in Table S2, ESI†), a consistent number of them is novel, and then possible peculiar of the neurotoxic phenotype of microglia we achieved by our experimental setup. Accordingly, we may propose the corresponding proteins as potential redox-based biomarkers of the microglia activated by beta amyloid, to be further validated by structural and functional studies *in vivo*.

Among the proteins selectively redox modified, three proteins were considered, namely peroxiredoxin-6 (Prdx6), Ras-related C3 botulinum toxin substrate 1 (Rac1) and chloride intracellular channel protein 1 (CLIC1), each of them representative of a link between oxidative stress and microglial neurotoxic activity.

In the case of Prdx6, the cysteine residue we detected (Cys47) is indeed known to be involved in the active site as a free thiol, and forming a transient adduct with the GSH during the enzyme turnover.[44] The selective enrichment of the peptide encompassing the Cys47 only in the activated microglia proved that under an amyloid injury the reversible redox modified form of the active cysteine is prevalent, and thus that in these conditions Prdx6 enhances its catalytic turnover. According to this scenario, Prdx6 should be considered an actor with a protective role against the oxidative stress in microglia, cooperating to sustain the transition toward a chronic neuroinflammatory phenotype and reinforce the role of this protein in AD. Indeed, an engagement of Prdx6 in the AD has been recently proposed by two different groups in neuronal cell cultures and transgenic mice, although opposite effects of its over-expression have been observed.[45, 46]

The other interesting protein of the microglia redox proteome is Rac1, a small GTPase belonging to the Rho GTPase family, that in its active form can bind different protein effectors related to secretory pathways, phagocytosis and apoptosis.[47] Rac1 represents, alternatively with the isoform Rac2 and together with p40phox, p47phox and p67phox, the cytosolic regulatory subunit of the NADPH oxidase complex.[48, 49] In the resting microglial status, inactive GDP-bound Rac1 are sequestered in the cytosol by Rho GDP-dissociation inhibitor (RhoGDI); conversely after microglia activation, Rac1 is activated through GTP binding, dissociates from RhoGDI and translocates to the plasma membrane where contributes to NADPH oxidase activation.[50] We found a selective

enrichment of RRM of Rac1 on Cys105, already annotated as nitrosylated.[51] A role of RRM in enhancing GTP binding has been reported by *in vitro* studies for the alternative Rac2 isoform,[52] that conversely we found redox modified both in treated and in untreated microglial cells (Table S1, ESI†). Hence, our data confirm that Cys105 is a sensitive site on Rac1 toward oxidative stress, and suggest that, in microglia, redox modified-Rac1 may relate with activation of NADPH oxidase. Finally, another relevant protein which appears to be differently redox modified in the beta amyloid treated microglia respect to control, is CLIC1, a member of the chloride channel protein family. Proteins belonging to this family are involved in many physiological processes such as cell division, cell cycle and apoptosis, cell differentiation, and also in pathophysiological processes such as neurodegenerative diseases and different types of cancer.[reviewed in 53] Among these proteins CLIC1 has been reported to undergo a "metamorphic" transition from a soluble to an integral membrane form upon oxidative stress.[54, 55] Once into the plasma membrane, CLIC1 can oligomerize, forming an ion channel for the influx of chloride ions altering the membrane ionic conductance.[56, 57] Treatment of microglial cells with amyloid induces its localization on the plasma membrane, and CLIC1 silencing alters both the release of TNF-α and ●NO production.[56] Moreover, blockade of CLIC1 stimulates amyloid phagocytosis in mononuclear phagocytes.[58] Recently, it has been proposed that CLIC1 could modify macrophage activity through the modulation of phagosomal acidification.[59] Structural studies on CLIC1 reported that the incubation with hydrogen peroxide leads to the formation of an intramolecular disulfide bridge between Cys24 and Cys59, triggering a conformational transition toward a dimer able to colonize a lipid bilayer.[55, 60, 61] In our analysis, we actually identified peptide encompassing Cys24 by shotgun proteomics of the peptide mixture enriched by biotin switch only upon amyloid stimulation, but with a very low level of reproducibility among the biological and technical replica we independently processed by shotgun proteomics (data not shown). Conversely, the enrichment of the peptide encompassing Cys191 we observed in activated microglia strongly suggests a possible novel role for this site in the transition of CLIC1 toward the acquisition of the dimeric structure. Interestingly, in a very recent and robust

screening of S-nitrosylation sites on the human proteome, the same cysteinyl residue has been found modified.[62] This data reinforces our hypothesis on the role of Cys191 in the peculiar functions of the highly structurally conserved CLIC1 proteins, in which 98.3% residues out of 241 overlapping are identical between human and mouse.

Conclusion

Nowadays, an effort is made to deciphering rules of thiol-based switches in a genome-wide manner.[62-64] The "biotin switch" and the shotgun proteomics we applied in this study yielded a consistent list of peptide sequences encompassing cysteinyl residues that we pinpointed as sensitive toward redox modifications. The list here reported will provide reliable data for bioinformatics to better refine the knowledge of the physico-chemical features that in proteins constitute the consensus motif for RRMs.

Through this site-specific proteomics approach employed, we were able to successfully infer reversible redox post-translational modifications on target proteins possibly involved in the microglia neuroinflammation phenotype. In our previous studies, we highlighted by expression proteomics that only one protein up- and few proteins down-regulated after $A\beta_{25-35}$ treatment.[11] Here, we observed that few but critical cellular processes are targeted by RRM modification induced by the amyloid treatment. Taken together, these two studies do suggest that the activation of microglia by amyloid is based more on redox post-translational modification activity, fast and selective, rather than on transcriptional modulation. Moreover, for at least two of the proteins identified in this paper, namely Prdx6 and Rac1, we were able to suggest mechanisms through which RRM could affect the peculiar microglia role in the amyloidogenic injury, that is at the same time to reinforce the oxidative burst and to resist toward it. Furthermore, the RRM modulation we observed on CLIC1 reinforces the structural and functional relationships between oxidative stress and its metamorphic transition from a soluble to an integral membrane form.

In our survey, novel RRM protein targets emerged with respect to those already identified in the neuronal compartment. A deeper analysis of the involvement of these proteins in microglia activation could disclose further relationships between the oxidative stress and the molecular basis of cell functions and dysfunctions in the neural tissue.

Acknowledgments

This work has been partly supported by an Italian grant from MIUR (to MES; grant number PRIN 2010HEBBB8_002), by a grant of Sapienza University (to MES; grant number C26A124WCR). The funders had no role in study design, data collection and analysis, decision to publish, or preparation of the manuscript. None of the authors have competing interests to declare.

References

1. M. Goedert and M. G. Spillantini, *Science,* 2006, **314**, 777-781.
2. C. Ballard, S. Gautheier, A. Corbett, C. Brayne, D. Aarsland and E. Jones, *Lancet*, 2011, **377**, 1019-1031.
3. C. Haass and D. J. Selkoe, *Nat. Rev. Mol. Cell Biol.*, 2007, **8**, 101-112.
4. R. Rodrigues, R. B. Petersen and G. Perry, *Cell. Mol. Neurobiol.*, 2014, **34**, 925-949.
5. H. L. Hsieh and C. M.Yang, *Biomed. Res. Int.*, 2013, **2013**, 484613.
6. V. H. Perry and C. Holmes, *Nat. Rev. Neurol.*, 2014, **10**, 217-224.
7. H. M. Gao, H. Zhou and J. S. Hong, *Trends Pharmacol. Sci.*, 2012, **33**, 295-303.
8. H. Kettenmann, U. K. Hanisch and M. Noda, A. Verkhratsky, *Physiol. Rev.*, 2011, **91**, 461-553.
9. M. K. Jha, J. H. Kim and K. Suk, *Proteomics*, 2014, **14**, 378-398.
10. D. P. Schafer, E. K. Lehrman and B. Stevens, *Glia*, 2013, **61**, 24-36.

11. L. Di Francesco, V. Correani, C. Fabrizi, L. Fumagalli, M. Mazzanti, B. Maras and M. E. Schininà, *Proteomics*, 2012, **12**, 124-134.
12. J. Gimeno-Baygon, A. Lapez-Lapez, M. J. Rodraguez and N. Mahy, *J. Neurosci. Res.*, 2014, **92**, 723-731.
13. R. Requejo, T. R. Hurd, N. J. Costa and M. P. Murphy, *FEBS J.*, 2010, **277**, 1465-1480.
14. B. Groitl and U. Jakob, *Biochim. Biophys. Acta*, 2014, **1844**, 1335-1343.
15. T. Nakamura, D. H. Cho and S. A. Lipton, *Exp. Neurol.*, 2012, **238**, 12-21.
16. C. L. Grek, J. Zhang, Y. Manevich and D. M. Townsend, K. D. Tew, *J. Biol. Chem.*, 2013, **288**, 26497-26504.
17. I. Dalle-Donne, R. Rossi, G. Colombo, D. Giustarini and A. Milzani, *Trends Biochem. Sci.*, 2009, **34**, 85-96.
18. J. J. Mieyal, M. M. Gallogly, S. Qanungo, E. A. Sabens and M. D. Shelton, *Antioxid. Redox Signaling*, 2008, **10**, 1941-1988.
19. E. A. Sabens Liedhegner, X. H. Gao and J. J. Mieyal, *Antioxid. Redox Signaling*, 2012, **16**, 543-566.
20. T. Nakamura, S. Tu, M. W. Akhtar, C. R. Sunico, S. Okamoto and S. A. Lipton, *Neuron*, 2013, **78**, 596-614.
21. S. F. Newman, R. Sultana, M. Perluigi, R. Coccia, J. Cai, W. M. Pierce, J. B. Klein, D. M. Turner and D. A. Butterfield, *J. Neurosci. Res.*, 2007, **85**, 1506-1514.
22. C. Zhang, C. C. Kuo, A. W. Chiu and J. Feng, *J. Alzheimers Dis.*, 2012, **30**, 919-934.
23. Q. F. Zhao, J. T. Yu and L. Tan, *Mol. Neurobiol.*, 2014, DOI: 10.1007/s12035-014-8672-2.
24. Y. M. Go and D. P. Jones, *J. Biol. Chem.,* 2013, **288**, 26512-26520.
25. B. McDonagh, S. Ogueta, G. Lasarte, C. A. Padilla and J. A. Bárcena, *J. Proteomics*, 2009, **72**, 677-689.
26. E. Blasi, R. Barluzzi, V. Bocchini, R. Mazzolla and F. Bistoni, *J. Neuroimmunol.*, 1990, **27**, 229-237.

27. L. Millucci, R. Raggiaschi, D. Franceschini, G. Terstappen and A. Santucci, *J. Biosci.*, 2009, **34**, 293-303.

28. J. Rappsilber, M. Mann and Y. Ishihama, *Nat. Protoc.*, 2007, **2**, 1896-1906.

29. J. Cox and M. Mann, *Nat. Biotechnol.*, 2008, **26**, 1367-1372.

30. K. Mann and M. Mann, *Proteome Sci.*, 2011, **9**, 7.

31. G. Mermelekas, M. Makridakis, T. Koeck and A. Vlahou, *Expert Rev. Proteomics*, 2013, **10**, 537-549.

32. S. E. Leonard and K. S. Carroll, *Curr. Opin. Chem. Biol.*, 2011, **15**, 88-102.

33. S. Ratnayake, I. H. Dias, E. Lattman and H. R. Griffiths, *J. Proteomics*, 2013, **92**, 160-170.

34. J. Guo, M. J. Gaffrey, D. Su, T. Liu, D. G. 2nd Camp and R. D. Smith, W. J. Qian, *Nat. Protoc.*, 2014, **9**, 64-75.

35. M. Zaccarin, M. Falda, A. Roveri, V. Bosello-Travain, L. Bordin, M. Maiorino, F. Ursini and S. Toppo, *Free Radic. Bio. Med.*, 2014, **71**, 90-98.

36. A. Henn, S. Lund, M. Hedtjarn, A. Schrattenholz, P. Porzgen and M. Leist, *ALTEX*, 2009, **26**, 83-94.

37. D. Han, S. Moon, Y. Kim, J. Kim, J. Jin, Y. Kim, *Proteomics*, 2013, **13**, 2984-2988.

38. S. Varadarajan, J. Kanski, M. Aksenova, C. Lauderback and D. A. Butterfield, *J. Am. Chem. Soc.*, 2001, **123**, 5625-5631.

39. S. Martire, A. Fuso, D. Rotili, I. Tempera, C. Giordano, I. De Zottis, A. Muzi, P. Vernole, G. Graziani, E. Lococo, M. Faraldi, B. Maras, S. Scarpa, L. Mosca and M. D'Erme, *PLoS One*, 2013, **8**, e72169.

40. V. K. Sonkar, P. P. Kulkarni and D. Dash, *FASEB J.*, 2014, **28**, 1819-1829.

41. R. Ghasemi, A. Zarifkar, K. Rastegar, N. Maghsoudi and M. Moosavi, *Eur. J. Pharmacol.*, 2014, **726C**, 33-40.

42. A. Khan, K. Vaibhav, H. Javed, R. Tabassum, M. E. Ahmed, M. M. Khan, M. B. Khan, P. Shrivastava, F. Islam, M. S. Siddiqui, M. M. Safhi and F. Islam, *Neurochem. Res.*, 2014, **39**, 344-352.

43. D. Su, M. J. Gaffrey, J. Guo, K. E. Hatchell, R. K. Chu, T. R. Clauss, J. T. Aldrich, S. Wu, S. Purvine, D. G. Camp, R. D. Smith, B. D. Thrall and W. J. Qian, *Free Radic. Bio. Med.*, 2014, **67**, 460-470.

44. Y. Manevich, S. I. Feinstein and A. B. Fisher, *Proc. Natl. Acad. Sci. U.S.A.*, 2004, **101**, 3780-3785.

45. I. K. Kim, K. J. Lee, S. Rhee, S. B. Seo and J. H. Pak, *Free Radical Res.*, 2013, **47**, 836-846.

46. H. M. Yun, P. Jin, J. Y. Han, M. S. Lee, S. B. Han, K. W. Oh, S. H. Hong, E. Y. Jung and J. T. Hong, *Mol. Neurobiol.*, 2013, **48**, 941-951.

47. T. R. Stankiewicz and D. A. Linseman, Front. Cell. Neurosci., 2014, 8, 314.

48. N. D'Ambrosi, S. Rossi, V. Gerbino and M. Cozzolino, *Front. Cell. Neurosci.,* 2014, **8**, 279.

49. B. M. Babior, *Blood*, 1999, **93**, 1464-1476.

50. B. L. Wilkinson and G. E. Landreth, *J. Neuroinflamm.*, 2006, **3**, 30.

51. Y. J. Chen, W. C. Ku, P. Y. Lin, H. C. Chou, K. H. Khoo and Y. J. Chen, *J. Proteome Res.*, 2010, **9**, 6417-6439.

52. I. S. Kil, S. W. Shin and J. W. Park, *Biochem. Biophys. Res. Commun.*, 2012, **425**, 892-896.

53. H. Singh, *FEBS Letters*, 2010, **584**, 2112-2121.

54. D. R. Littler, S. J. Harrop, S- C. Goodchild, J. M. Phang, A. V. Mynott, L. Jiang, S. M. Valenzuela, M. Mazzanti, L. J. Brown, S. N. Breit, P. M. G. Curmi, *FEBS Letters*, 2010, **584**, 2093-2101.

55. D. R. Littler, S. J. Harrop, W. D. Fairlie, L. J. Brown, G. J. Pankhurst, S. Pankhurst, M. Z. DeMaere, T. J. Campbell, A. R. Bauskin, R. Tonini, M. Mazzanti, S. N. Breit and P. M. Curmi, *J. Biol. Chem.*, 2004, **279**, 9298-9305.

56. G. Novarino, C. Fabrizi, R. Tonini, M. A. Denti, F. Malchiodi-Albedi, G. M. Lauro, B. Sacchetti, S. Paradisi, A. Ferroni, P. M. Curmi, S. N. Breit and M. Mazzanti, *J. Neurosci.*, 2004, **24**, 5322-5330.

57. B. M. Tulk, S. Kapadia and J. C. Edwards, *Am. J. Physiol.-Cell. Ph.*, 2002, **282**, C1103-1112.

58. S. Paradisi, A. Matteucci, C. Fabrizi, M. A. Denti, R. Abeti, S. N. Breit, F. Malchiodi-Albedi and M. Mazzanti, *J. Neurosci. Res.*, 2008, **86**, 2488-2498.

59. L. Jiang, K. Salao, H. Li, J. M. Rybicka, R. M. Yates, X. W. Luo, X. X. Shi, T. Kuffner, V. W. Tsai, Y. Husaini, L. Wu, D. A. Brown, T. Grewal, L. J. Brown, P. M. Curmi and S. N. Breit, *J. Cell Sci.*, 2012, **125**, 5479-5488.

60. S. C. Goodchild, M. W. Howell, N. M. Cordina, D. R. Littler, S. N. Breit, P. M. Curmi and L. J. Brown, *Eur. Biophys. J. Biophys. Lett.,* 2009, **39**, 129-138.

61. S. C. Goodchild, M. W. Howell, D. R. Littler, R. A. Mandyam, K. L. Sale, M. Mazzanti, S. N. Breit and P. M. Curmi, L. J. Brown, *Biochemistry*, 2010, **49**, 5278-5289.

62. Y. I. Lee, D. Giovinazzo, H. C. Kang, Y. Lee, J. S. Jeong, P. T. Doulias, Z. Xie, J. Hu, M. Ghasemi, H. Ischiropoulos, J. Qian, H. Zhu, S. Blackshaw, V. L. Dawson and T. M. Dawson, *Mol. Cell. Proteomics*, 2014, **13**, 63-72.

63. C. Sun, Z. Z. Shi, X. Zhou, L. Chen and X. M. Zhao, *PLoS One*, 2013, **8**, e55512.

64. Y. J. Chen, C. T. Lu, T. Y. Lee and Y. J. Chen, *Bioinformatics*, 2014, **pii**, btu301.

65. M. Liu, J. Hou, L. Huang, X. Huang, T. H. Heibeck, R. Zhao, L. Pasa-Tolic, R. D. Smith, Y. Li, K. Fu, Z. Zhang, S. H. Hinrichs and S. J. Ding, *Anal. Chem.*, 2010, **82**, 7160-7168.

66. J. S. Paige, G. Xu, B. Stancevic and S. R. Jaffrey, *Chem. Biol.*, 2008, **15**, 1307-1316.

67. H. Ye, B. Li, V. Subramanian, B. H. Choi, Y. Liang, A. Harikishore, G. Chakraborty, K. Baek and H. S. Yoon, *Biochim. Biophys. Acta*, 2013, **1828**, 1083-1093.

68. R. Scheving, I. Wittig, H. Heide, B. Albuquerque, M. Steger, U. Brandt and I. Tegeder, *J. Proteomics*, 2012, **75**, 3987-4004.

69. Y. W. Lam, Y. Yuan, J. Isaac, C. V. Babu, J. Meller and S. M. Ho, *PLoS One*, 2010, **5**, e9075.

70. D. Tello, C. Tarín, P. Ahicart, R. Bretón-Romero, S. Lamas and A. Martínez-Ruiz, *Proteomics*, 2009, **9**, 5359-5370.

Figure Capture

Fig. 1. - **Workflow of the differential analysis of the reversible redox modified proteome**. Reversible redox modified cysteinyl residues of the protein extracts from BV2 cell lines $A\beta_{25-35}$ treated (microglia + $A\beta_{25-35;}$ three biological replicates) and untreated (resting microglia; three biological replicates) were specifically labelled with a biotinyl bait as described in Material and Methods. Peptide digests were obtained by trypsin treatment, and biotinyl-labelled peptides selectively recovered by a streptavidin-fishing. Two technical replica derived from each fished mixture were subjected to identification by mass spectrometry. A total of 12 LC-MS/MS experiments were performed. We considered only peptides uniquely assigned to one protein and identified in at least one technical replica of all the three biological replicates of the microglia cultures used.

Fig. 2 – Effects of $A\beta_{25-35}$ on BV2 cells. (A) Induction of TNF-α in BV2 cells treated for 4 h with 50 μM $A\beta_{25-35}$; TNF-α mRNA was detected by RT-PCR in $A\beta_{25-35}$ untreated (-) and treated (+) cells. The mRNA for GAPDH was used as reference. (B) Detection of the cytokine-inducible isoform of the nitric oxide synthases (iNOS) in BV2 cells treated for 24 h with 50 μM $A\beta_{25-35}$; iNOS was immunodetected in $A\beta_{25-35}$ untreated (-) and treated (+) cells. β-Tubulin was used as reference. (C) Cell viability in BV2 treated for 24 h with 50 μM $A\beta_{25-35}$; viability was assessed by measuring LDH released in the culture medium. Values are expressed as percentage with respect to those obtained by lysing cells with detergent 2% Triton X-100. Ctrl, $A\beta_{25-35}$ untreated cell; $A\beta_{25-35,}$ 50 μM $A\beta_{25-35}$ treated; TX100, cells lysed by treatment with Triton X-100.

Fig. 3 - Analysis of proteins found reversibly redox modified in BV2 cells. Microglia proteome components found to be redox modified on cysteinyl residues were clustered for function (Panel A) and biological processes (Panel B) respectively, according to the Ingenuity Pathways Knowledge

Bases (IPA). The enrichment of selected biological processes has been evaluated by IPA algorithm through Fisher's exact test, and reported in panel B, as –log (P value).

Fig. 4 - Expression levels of selected redox modified proteins. On the left: immunodetection of Rac1, CLIC1 and Prdx6 in $A\beta_{25-35}$ treated (+) and untreated (-) cells. All the three independent cell preparations are reported. On the right: relative intensities of the optical densities of each the three protein bands and the corresponding GAPDH band. Quantitative data are expressed as percentage in respect to the ratio value determined in the untreated cells. Data were collected from independent cell preparations (n=3), and averaged (±SD). Statistical analysis was performed by T-student test. p-value of <0.01 were considered statistically significant.

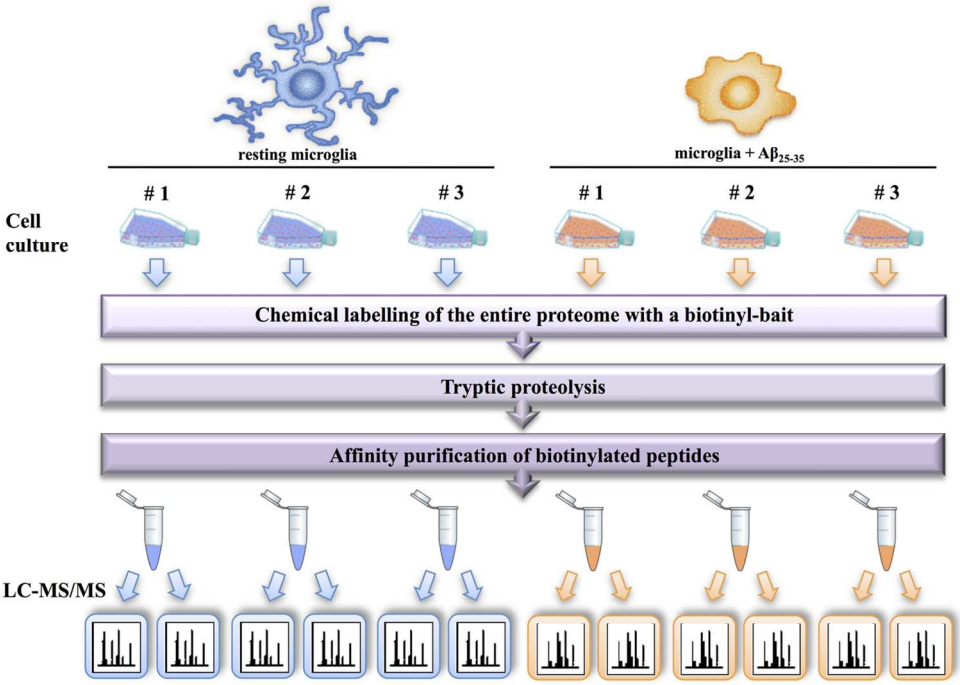

129x98mm (300 x 300 DPI)

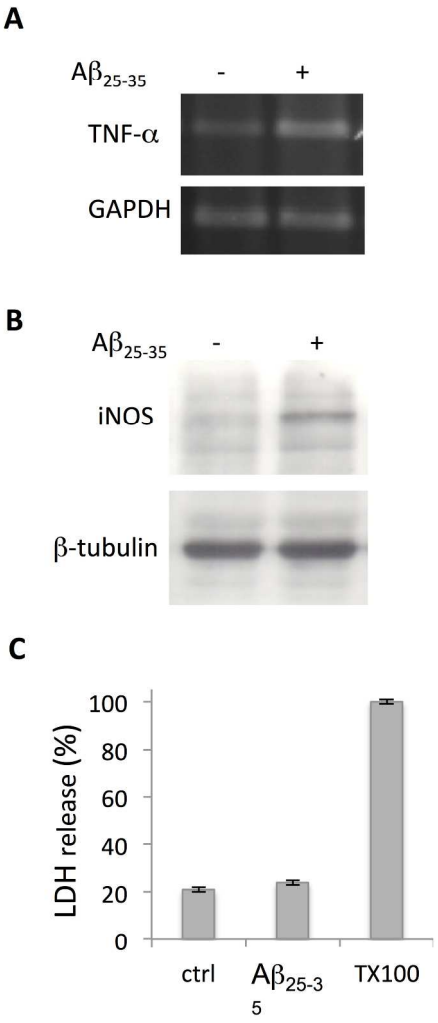

179x390mm (300 x 300 DPI)

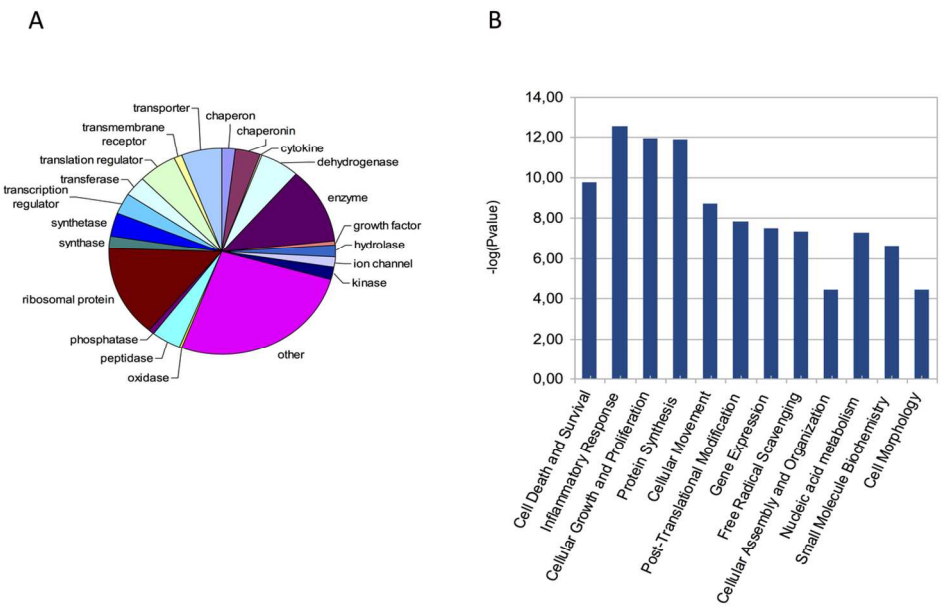

119x84mm (300 x 300 DPI)

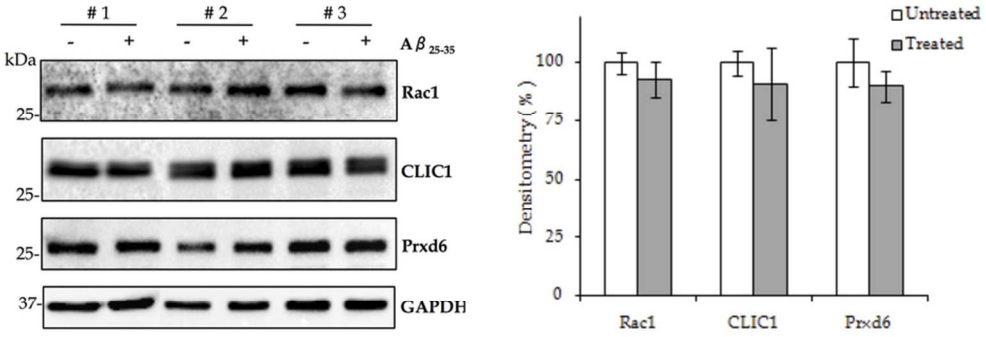

79x37mm (300 x 300 DPI)

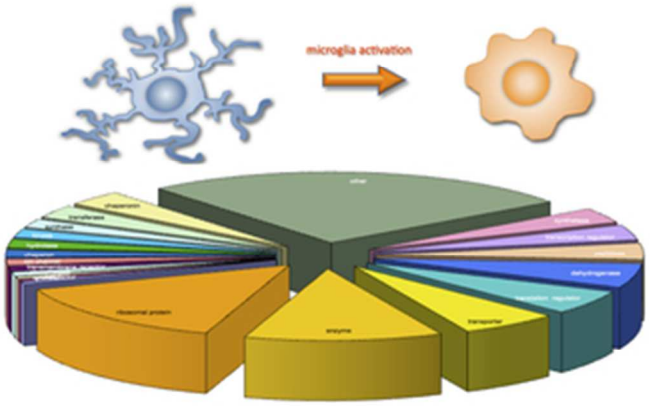

Reversible redox modifications of the microglia proteome contribute to switch these neuronal sentinel cells toward a neuroinflammatory phenotype.
39x19mm (300 x 300 DPI)

Table S2

Summary of reversible redox modified cysteinyl sites changing in microglia proteins upon treatment with $A\beta_{25-35}$ peptide.

Proteins[a]	Protein names	RRM containing peptide sequence[b]	PEP[c]	Score[d]	Redox sensitive site[e]			RRM annotation[f]
					Cys#	resting	activated	
Q9QZB7	Actin-related protein 1	SVATLILDSLLQCPIDTR	7.85E-007	157.8	291	+		
P50247	Adenosylhomocysteinase	VIITEIDPINALQAAMEGYEVTTMDEACK	6.50E-014	181.24	266	+		
P47738	Aldehyde dehydrogenase	LLCGGGAAADR	1.37E-048	145.55	388		+	
Q9D0I9	Arginine-tRNA ligase, cytoplasmic	LQEVFGCAIR	4.82E-003	97.456	86		+	SSG[43]
Q922B2	Aspartate-tRNA ligase, cytoplasmic	VFCIGPVFR	9.16E-006	143.85	267		+	
Q9DCX2	ATP synthase subunit d	SCAEFVSGSQLR	5.01E-032	259.47	101		+	
Q80WV3	Carbohydrate sulfotransferase 2	KEGMGGPADYHALGAMEVICNSMAK	4.09E-002	38.175	399	+		
O70370	Cathepsin S	LISLSAQNLVDCSNEEK	9.52E-122	414.82	178		+	SSG[43]
Q9WUU7	Cathepsin Z	HGIPDETCNNYQAK	2.18E-015	221.86	156		+	SSG[43]
Q9Z1Q5	Chloride intracellular channel protein 1	LHIVQVVCK	6.28E-006	149.65	191		+	SNO[62, 65]
P18760	Cofilin-1	HELQANCYEEVKDR	2.01E-067	328.14	139		+	SSG[43] SNO[62, 65, 66]
O08749	Dihydrolipoyl dehydrogenase	VCHAHPTLSEAFR	1.82E-003	108.72	484		+	
Q9Z0J0	Epididymal secretory protein E1	SGINCPIQK	2.75E-002	57.96	99		+	
P51906	Excitatory amino acid transporter 3	NMFPENLVQACFQQYK	3.87E-002	36.993	158	+		
P06745	Glucose-6-phosphate isomerase	MIPCDFLIPVQTQHPIR	3.98E-002	40.242	404		+	SSG[43]
P68040	Guanine nucleotide-binding protein subunit beta-2-like 1	AEPPQCTSLAWSADGQTLFAGYTDNLVR	3.11E-003	76.152	286	+		SSG[43]
		LWNTLGVCK	2.56E-004	117.89	138		+	SSG[43]
Q8BG05	Heterogeneous nuclear ribonucleoprotein A3	WGTLTDCVVMR	7.20E-003	97.734	64		+	SNO[51]
Q9Z2X1	Heterogeneous nuclear ribonucleoprotein F	YGDSEFTVQSTTGHCVHMR	1.05E-005	138.05	290		+	
O35737	Heterogeneous nuclear ribonucleoprotein H	GLPWSCSADEVQR	9.79E-005	142.38	22		+	
P61979	Heterogeneous nuclear ribonucleoprotein K	IIPTLEEGLQLPSPTATSQLPLESDAVECLNYQHYK	2.03E-012	141.43	132	+		SSG[43]
		LFQECCPHSTDR	4.53E-003	99.283	185[g]		+	SNO[51]
Q8R081	Heterogeneous nuclear ribonucleoprotein L	VFNVFCLYGNVEK	2.03E-031	267.67	401	+		SNO[51]
		LCFSTAQHAS	1.42E-011	205.18	578		+	SSG[43]

P21956	Lactadherin	ITLRLELLGC	3.73E-010	130.98	463	+		SS with 308[67]
Q3V3R1	Monofunctional C1-tetrahydrofolate synthase	EAGLDITHICLPPDSGEDEIIDEILK	4.04E-002	38.237	129	+		SSG[43]
Q922Q1	MOSC domain-containing protein 2	CVLTTVDPDTGIIDR	3.98E-002	43.813	274	+		
Q7TPV4	Myb-binding protein 1A	SVFGHICPHLTPR	9.99E-004	124.21	676		+	SNO[51]
O08709	Peroxiredoxin-6	DFTPVCTTELGR	1.79E-031	169.65	47		+	SSG[43, 44] SNO[65, 66, 68]
Q9WUA3	6-phosphofructokinase	LGITNLCVIGGDGSLTGANLFR	2.83E-027	240.71	122	+		
Q9DCD0	6-phosphogluconate dehydrogenase, decarboxylating	SAVDNCQDSWR	5.00E-024	250.7	402		+	
Q9DBJ1	Phosphoglycerate mutase 1	YADLTEDQLPSCESLK	1.05E-043	300.03	153		+	SSG[43] SNO[65, 66]
Q61233	Plastin-2	KLENCNYAVDLGK	1.71E-022	237.32	460		+	SSG[43]
P62962	Profilin-1	CYEMASHLR	2.90E-008	166.09	128		+	
P17918	Proliferating cell nuclear antigen	DLSHIGDAVVISCAK	1.54E-022	244.44	162		+	SSG[43] SNO[51, 65]
P50580	Proliferation-associated protein 2G4	AAHLCAEAALR	9.21E-006	137.95	149		+	
Q9R0Q7	Prostaglandin E synthase 3	LTFSCLGGSDNFK	2.68E-022	232.6	402		+	SSG[43] SNO[65]
Q9R1P4	Proteasome subunit alpha type-1	LLCNFMR	5.43E-003	103.29	85		+	SSG[43]
Q9CQ89	Protein CutA	LAACVNLIPQITSIYEWK	6.06E-003	86.367	94	+		
P27773	Protein disulfide-isomerase A3	FIQDSIFGLCPHMTEDNKDLIQGK	5.48E-012	177.73	244		+	SNO[69] SSG[43]
E9PZD9	Protein E330020D12Rik	AQGQRPCGFR	3.42E-002	45.161	49	+		
E9Q8I7	Protein Nfxl1	KCCPGNCPPCDQNCGR	4.25E-002	26.292	492/493/ 497/500[h]		+	
P52480	Pyruvate kinase isozymes M1/M2	AEGSDVANAVLDGADCIMLSGETAKGDYPLEAVR	2.65E-027	219.26	358	+		SSG[43]
P63001	Ras-related C3 botulinum toxin substrate 1	HHCPNTPIILVGTK	1.15E-002	74.475	105		+	SNO[51]
Q91VI7	Ribonuclease inhibitor	SLLELQMSSNPLGDEGVQELCK	2.17E-036	276.68	357	+		
Q5XJF6	Ribosomal protein	FSVCVLGDQQHCDEAK	1.34E-011	203.7	74[g]		+	
P47962	60S ribosomal protein L5	IEGDMIVCAAYAHELPK	2.05E-004	119.65	76		+	SSG[43]
P62918	60S ribosomal protein L8	AQLNIGNVLPVGTMPEGTIVCCLEEKPGDR	6.11E-005	107.17	114/115[h]	+		
P35979	60S ribosomal protein L12	EILGTAQSVGCNVDGR	5.11E-031	261.64	141		+	SSG[43]

P62830	60S ribosomal protein L23	ECADLWPR	7.07E-003	72.485	125		+	SSG[43]
P14115	60S ribosomal protein L27a	NQSFCPTVNLDK	1.65E-022	232.5	70		+	
P83882	60S ribosomal protein L36a	LECVEPNCR	8.84E-005	134.26	72[g]		+	
Q9R0P3	S-formylglutathione hydrolase	CPALYWLSGLTCTEQNFISK	2.26E-003	99.891	56[g]	+		
O55143	Sarcoplasmic/endoplasmic reticulum calcium ATPase 2	CHQYDGLVELATICALCNDSALDYNEAK	3.75E-002	36.142	417[g]	+		
Q9CZN7	Serine hydroxymethyltransferase	YYGGAEVVDEIELLCQR	3.05E-004	115.68	119	+		
Q6PDM2	Serine/arginine-rich splicing factor 1	EAGDVCYADVYR	1.07E-006	172.13	148		+	
P80316	T-complex protein 1 subunit epsilon	ETGANLAICQWGFDDEANHLLLQNGLPAVR	7.28E-008	135.54	302	+		
P80318	T-complex protein 1 subunit gamma	IPGGIIEDSCVLR	2.17E-010	200.93	213		+	SSG[43] SNO[51, 69]
		TLIQNCGASTIR	7.10E-144	265.22	455		+	SSG[43] SNO[51]
Q9R233	Tapasin	VSLTPAPVVWAAPGEAPPELLCLASHFFPAEGLEVK	5.96E-010	138.41	318	+		
Q921F2	TAR DNA-binding protein 43	VTEDENDEPIEIPSEDDGTVLLSTVTAQFPGACGLR	1.47E-002	63.203	39	+		
Q91WM3	U3 small nucleolar RNA-interacting protein 2	QLDPLCDIPLVGFINSLK	3.83E-009	173.98	416	+		
P62814	V-type proton ATPase subunit B, brain isoform	SDFEENGSMDNVCLFLNLANDPTIER	5.28E-003	71.428	258	+		
P20152	Vimentin	QVQSLTCEVDALK	1.95E-005	158.58	328		+	SSG[43] SNO[51, 66, 70]

[a] UniProtKB protein identifier.

[b] Sequence of peptides identified by shotgun proteomics as containing cysteinyl residues specifically sensible to the $A\beta_{25-35}$ treatment in BV2 cells.

[c] Peptide Posterior Error Probability (PEP) score, calculated by MaxQuant algorithms; the smaller the PEP, the more certain is the identification of a peptide.

[d] Andromeda score for the best associated MS/MS spectrum allowing identification in the shotgun proteomics analysis.

[e] Specific cysteinyl residue proved to lose (+, in the resting cell column) or to gain (+, in the activated cell column) the RRM upon beta amyloid treatment.

[f] Literature references on post-translational modifications annotated up to now for each of specific cysteinyl residues proved in our work carrying RRM. SS, disulphide bridge; SSG, Mixed disulphide bridge with glutathione; SNO, nitrosothiols. Numbers refer to those in the Reference section of the manuscript.

[g] Indicates certain identification of the RRM site due to the presence in MS/MS spectra of discriminating ions.

[h] Indicates ambiguous RRM sites due to lack of discriminating ions.

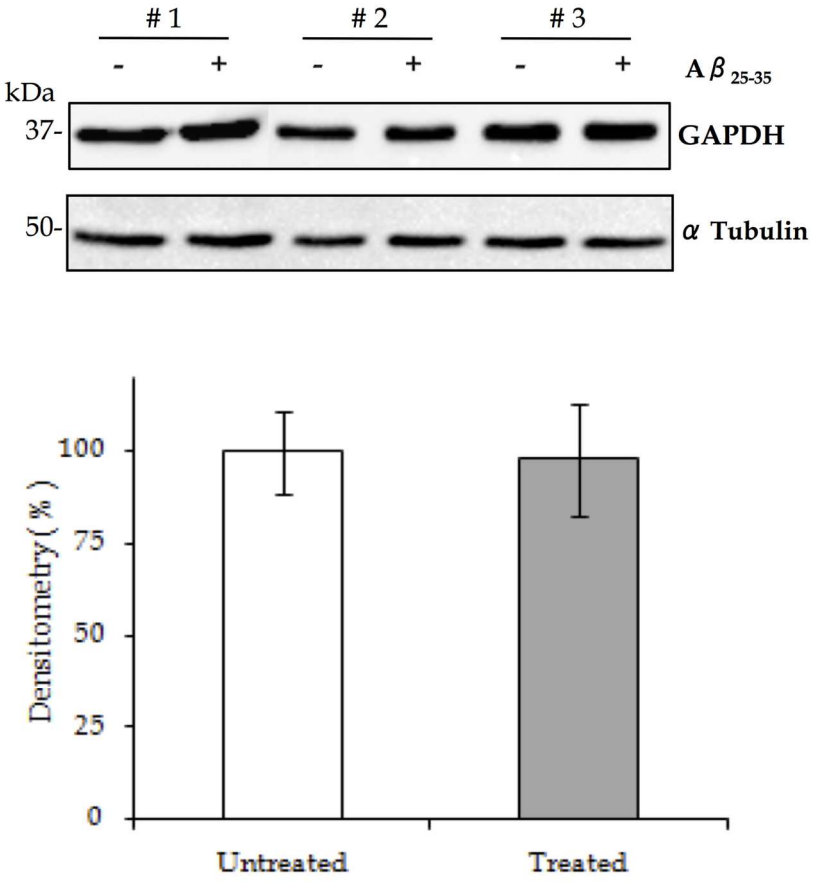

129x188mm (300 x 300 DPI)